Synthesis of Copper(I) Cyclic (Alkyl)(Amino)Carbene Complexes with Potentially Bidentate N^N, N^S and S^S Ligands for Efficient White Photoluminescence[†§]

Alexander S. Romanov, Florian Chotard, Jahan Rashid, and Manfred Bochmann*

School of Chemistry, University of East Anglia, Earlham Road, Norwich, NR4 7TJ, UK
e-mail: m.bochmann@uea.ac.uk

ORCID IDs:
Florian Chotard https://orcid.org/0000-0002-4791-5270
A. S. Romanov https://orcid.org/0000-0003-2617-6402
M. Bochmann https://orcid.org/0000-0001-7736-5428

Abstract

The reaction of (^{Me2}L)CuCl with either NaS_2CX [X = OEt, NEt_2 or carbazolate (Cz)] or with 1,3-diarylguanidine, 1,3-diarylformamidine or thioacetaniline in the presence of KO^{t}Bu affords the corresponding S- or N-bound copper complexes (^{Me2}L)Cu(S^S) **1**–**3**, (^{Me2}L)Cu(N^N) **4**/**5** and (^{Me2}L)Cu(N^S) **6** (aryl = 2,6-di*iso*propylphenyl; ^{Me2}L = 2,6-bis(*iso*propyl)phenyl-3,3,5,5-tetramethyl-2-pyrrolidinylidene). The crystal structure of (^{Me2}L)Cu(S_2CCz) (**3**) confirmed the three-coordinate geometry with S^S chelation and perpendicular orientation of the carbene and S^S ligands. On heating **3** cleanly eliminates CS_2 and forms (^{Me2}L)CuCz. The N-bound complexes show strongly distorted T-shaped (**4**) or undistorted linear (**5**) geometries. On excitation with UV light the S-bound complexes proved non-emissive, while the guanidinato and formamidinato complexes are strongly phosphorescent, with excited state lifetimes in the range of 11–24 µs in the solid state. The conformationally flexible formamidinato complex **5** shows intense green-white phosphorescence with a solid-state quantum yield of >96%.

Introduction

Linear coinage metal complexes of the type (L)MX based on L = cyclic (alkyl)(amino)carbene ligands (CAACs) have recently emerged as a novel class of light emitting materials due to their ability to act as highly efficient photoemitters in organic light-

emitting diodes (OLEDs).[1-11] In most cases the most efficient emitters proved to be complexes where X = aryl amide, and in particular X = carbazolate, giving rise to "carbene-metal-amide", or "CMA" materials. On photochemical or electrochemical excitation these compounds display highly efficient delayed emission, which is due to a charge transfer process involving electron donation from an electron-rich amide ligand to a LUMO based mainly on the carbene p-orbital, which acts as π-electron acceptor.[2,5,6,7,12-14] Numerous types of photoluminescent copper complexes are known which can show phosphorescence as well as efficient emission by thermally activated delayed fluorescence (TADF).[15] Here we report new types of CAAC copper complexes with different anionic ligands where X = bidentate xanthate, dithiocarbamate, guanidinate and formamidinate, in order to study the effect of coordinative variability and molecular flexibility on the photoemission properties. The copper formamidinato complex **5** proved to be a bright white-light emitter, with a near-unity solid state quantum yield.

Results and Discussion

Synthesis and Structures. Six new copper complexes of the type (^{Me2}L)Cu(S^S) **1**–**3**, (^{Me2}L)Cu(N^N) **4**/**5** and (^{Me2}L)Cu(N^S) **6** [^{Me2}L = ^{Me2}CAAC carbene, 2,6-bis(isopropyl)-phenyl-3,3,5,5-tetramethyl-2-pyrrolidinylidene] were prepared according to Scheme 1. Dithiocarbamate and xanthate ligands (S^S) were used as sodium or potassium salts, while for the guanidinate, formamidinate (N^N) and thioacetanilide (N^S) complexes the free ligands were reacted with (^{Me2}L)CuCl in the presence of KO^{t}Bu in diethyl ether. The desired products were obtained in high yields as brown (**1**), orange (**2**), red (**3**), yellow (**4** and **6**), and off-white (**5**) solids. Complexes **4** and **5** have excellent solubility in all common organic solvents but moderate solubility in hexane. Complexes **1**–**3** and **6** show poor solubility in hexane, moderate solubility in Et_2O, and good solubility in CH_2Cl_2. Complexes **1**–**3** are stable in air for at least several weeks whereas **4**–**6** are stable for several days in air and should be stored under argon. Their purity was established by ^{1}H and ^{13}C{^{1}H } NMR spectroscopy and elemental analysis after recrystallization.

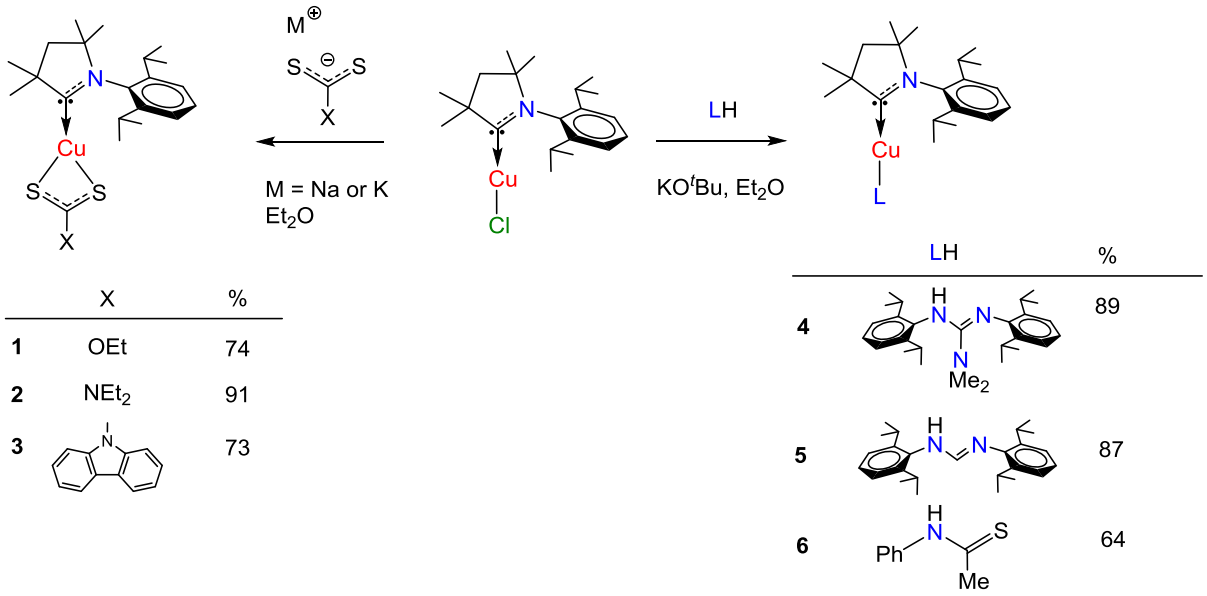

Scheme 1. Synthesis of copper complexes **1**–**6**.

The thermal stability of complexes **1**–**5** was assessed using thermogravimetric analysis (TGA, Figure 1) and differential scanning calorimetry (DSC). The copper S^S complexes are thermally labile. While complex **2** shows one step thermal decomposition (T_d, 5% weight loss at 202 °C), complexes **1** and **3** exhibit a two-step process starting at 158 °C with the loss of CS_2 in the first step. The CS_2 elimination process for **3** was confirmed by heating the compound to 180 °C under vacuum with a liquid nitrogen trap. Melting was observed at about 160 °C with a colour change of the melt from dark red to dark-brown after complete elimination of CS_2 under vacuum in 5 min, which was consistent with a mass loss. ^{1}H and $^{13}C\{^{1}H\}$ NMR characterization of the brown melt confirmed the complete conversion into the recently described[10] complex (^{Me2}L)Cu(carbazolate) (Scheme 2). The second decomposition occurs at about 216 and 284 °C for complexes **1** and **3**, respectively (Figure 1), similar to the behaviour of (CAAC)Cu(phenolate) and (CAAC)Cu(carbazolate) compounds.[2,3]

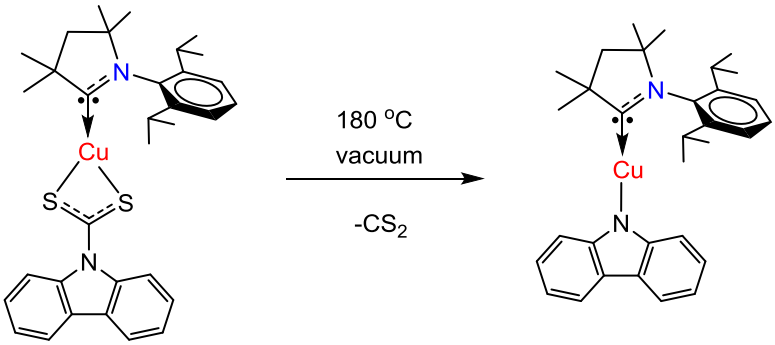

Scheme 2. Elimination of CS_2 from **3** on heating under vacuum.

Unlike the S^S complexes, the N^N complexes **4** and **5** proved significantly more stable: **4** melts above 220 °C and **5** above 200 °C without decomposition, which is only seen on further heating to 230 °C for **4** and 240 °C for **5**. Complex **4** shows decomposition in one step whereas the formamidinato complex **5** displays a two-step decomposition process. The first process can be associated with the loss of the ^{Me2}L ligand, which is consistent with the 40% mass loss, while the second process starts at 321 °C leading to quantitative evaporation of the crucible's content at 415 °C. Such thermal behaviour of complex **5** may find use as a stable precursor for the chemical vapour or atomic layer deposition (CVD or ALD) applications.[16]

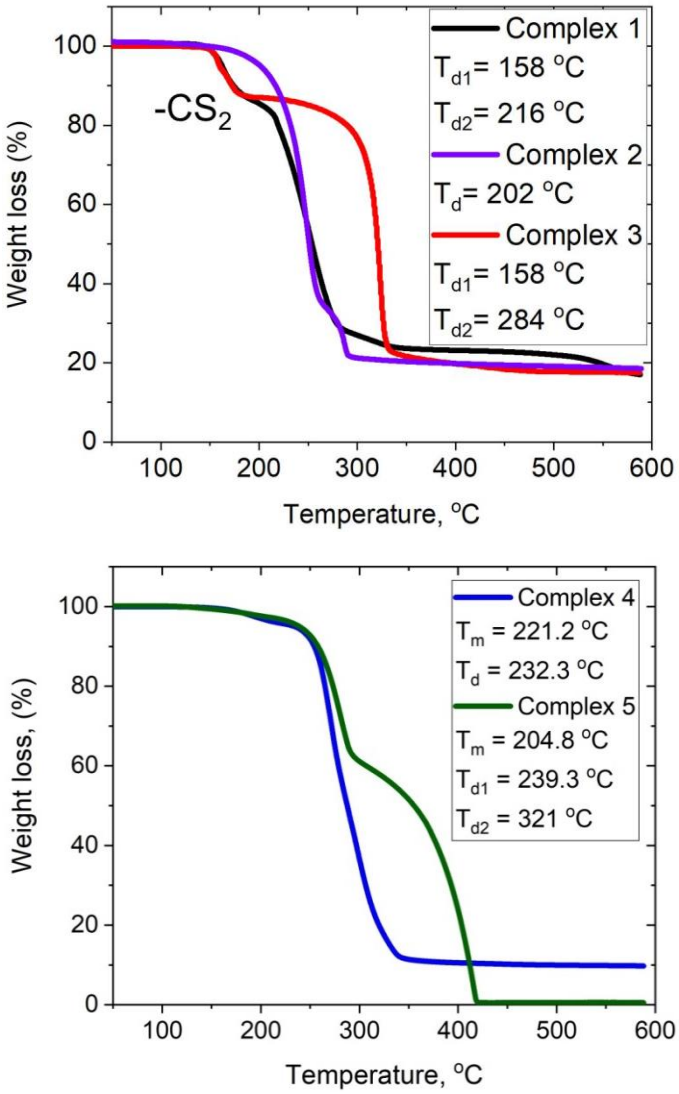

Figure 1. Thermogravimetric plots for S^S complexes **1** - **3** (top row) and the guanidinato and formamidinato complexes **4** and **5** (bottom row).

Crystals of (^{Me2}L)Cu(S_2CCz) (**3**) suitable for X-ray diffraction were obtained by layering CH_2Cl_2 solutions with hexane. Crystals of **4** and **5** were obtained by slow evaporation of the Et_2O solution under argon. All complexes are monomeric with one molecule in the unit cell. The crystal structure of **3** (Figure 2) shows that the complex is three-coordinate with a bidentate dithiocarbamate ligand. The Cu–$C_{carbene}$ bond length of 1.8772(17) Å is similar to ^{Me2}CAAC copper complexes synthesised previously.[2,3] The two Cu–S distances are nearly identical (Cu1–S1 2.3104(5), Cu1–S2 2.3166(5) Å). Whereas in (CAAC)metal carbazolate complexes the carbene and the carbazolate ligands are approximately co-planar,[2,3,7] in **3** the N1–C1–C2 and S1–C33–S2 planes form a dihedral angle of 94.4(1)° leading to almost perpendicular orientation of the two ligands. The four-membered CuS_2C cycle (Cu1–S1–C33–S2) has an envelope conformation with a dihedral angle of 21.6(1)° between S1-Cu1-S2 vs. S1-C33-S2. The Cz and CS2 moieties of the thiocarbamate ligand are coplanar, and there are weak intramolecular hydrogen bonding interactions C31–H31A···S1/ C22–H22A···S2 of 2.433(2)/2.438(1) Å with r(C–S) = 3.064(2)/3.074(2) Å and C–H–S angles of 125.1(1)/125.6(1)°.

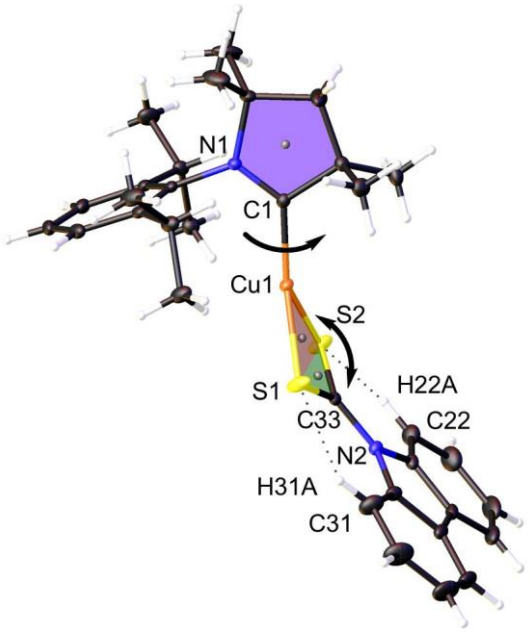

Figure 2. Crystal structure of (^{Me2}L)CuS_2CCz (**3**). Ellipsoids are shown at the 50% level. Selected bond lengths [Å] and angles [°]: Cu1–C1 1.8772(17), C1–N1 1.307(2), Cu1–S1 2.3104(5), Cu1–S1 2.3166(5), S1–C33 1.7045(18), S1–C33 1.7004(18); C1–Cu1–S1 140.35(5)°, C1–Cu1–S2 139.15(5)°. Dihedral angle N1–C1–C2/S1–C33–S2 94.4(1)°; S1-Cu1-S2/S1-C33-S2 21.6(1)°.

The guanidinate complex **4** (Figure 3) possesses a strongly distorted T-shaped geometry, with a short Cu1–N2 σ-bond of 1.8909(11) Å. The distance to the second N-atom is much longer, Cu1–N3 = 2.6725(11) Å; it is however 0.28 Å less than the sum of the Van der Waals radii for Cu(I) and N and consistent with a weak coordination to the metal centre. Such long Cu–N bonds have been reported before (2.66–2.74 Å).[17] The C1–Cu1–N2 moiety is linear, bond angle 171.56(6)°, whereas the C1–Cu1–N3 angle is 120.9(1)°. The three C33–N bond lengths are identical to ±0.03(1) Å and indicate extensive electron delocalisation in the guanidinate ligand. The C33–N3 bond length (1.3169(17) Å) is the shortest and likely affected by coordination with copper.

By contrast, the crystal structure of the formamidinato complex **5** (Figure 3) confirms a linear two coordinate geometry (C1–Cu1–N2 175.09(7)°) which, unlike **4**, lacks a close contact to the second nitrogen atom (Cu1–N3 2.912(14) Å). The Cu1–C1 and Cu1–N2 bond lengths are shorter by 0.01 and 0.03 Å for complex **5** compared with **4**, respectively. The carbon-nitrogen bond lengths in the formamidinato ligand are distinctly different from those in **4**, with long N2–C33 and short N3–C33 distances of 1.345(2) and 1.296(2) Å. These values are commensurate with localised C–N single and double bonds. The interplanar (twist) angles between the CAAC carbene (N1–C1–C2) and the amide ligands (N2–C33–N3) are 20.1(1)° and 27.4(2)° for **4** and **5**, respectively. The smaller Cu-carbene and Cu-amide distances coupled with the larger twist angle in **5** may have an impact on the photophysical properties in the solid state (*vide infra*).

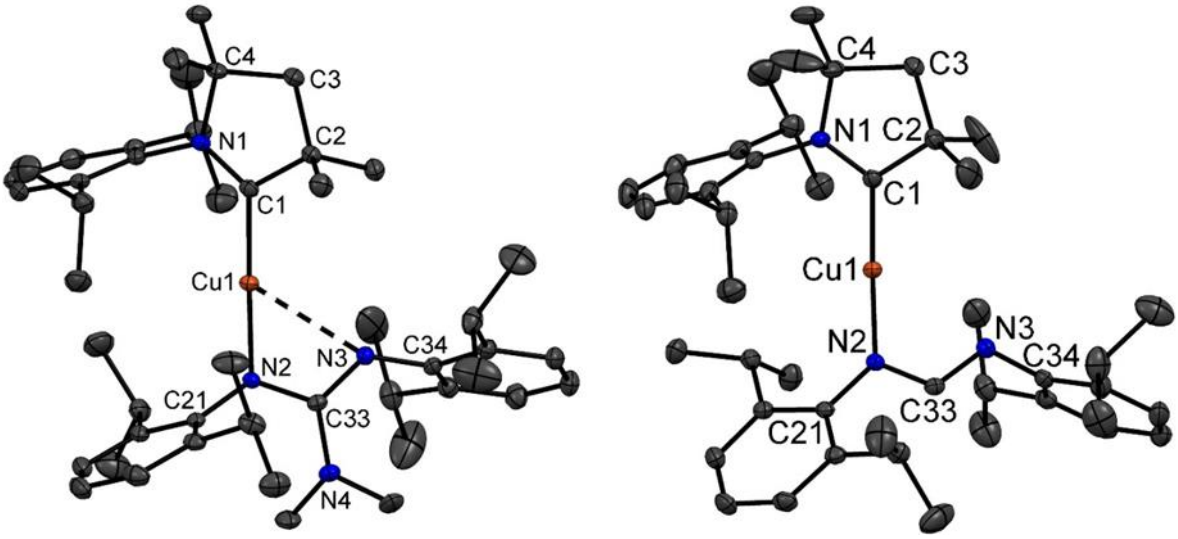

Figure 3. Crystal structures of **4** (left) and **5** (right). Ellipsoids are shown at the 50% level. Hydrogen atoms are omitted for clarity. Selected bond lengths [Å] and angles [°] for complex

4: Cu1–C1 1.8767(14), C1–N1 1.3012(18), Cu1–N2 1.8909(11), Cu1–N3 2.673(11), N2–C33 1.3563(17), N3–C33 1.3169(17), N4–C33 1.3898(17); C1–Cu1–N2 171.56(6). Complex **5**: Cu1–C1 1.8650(14), C1–N1 1.304(2), Cu1–N2 1.8650 (11), Cu1–N3 2.912 (14), N2–C33 1.345(2), N3–C33 1.296(2); C1–Cu1–N2 175.09(7).

Photophysical Properties. The UV/vis absorption spectra for copper complexes were collected in THF (Figure 4 and ESI, Table S1). All complexes show intra-ligand (IL) transitions of the CAAC carbene which can be ascribed to allowed π–π* transitions in the short wavelength region (260–270 nm) of the spectra. The S-bound complexes **1**–**3** and **6** possess a second absorption above 300 nm with a high extinction coefficient (>17,000 M^{-1} cm^{-1}) which suggest that it originates from another π–π* absorption located either in the thiocarbamate or thioanilide ligands. This was further supported by measuring UV-vis absorption in solvents with different polarity, for instance, complex 3 shows a small 67 meV blue shift on varying the solvent from toluene, THF and MeCN (see ESI, Fig. S1) while more than 300 meV blue-shift is common for ligand-to-ligand CT band in CMA emitters.[2,10] There is a 30 nm red-shift in the low energy absorption band on exchanging the xanthate ligand in **1** for dithiocarbamate in **3**. The UV/vis spectrum of the S^N complex **6** is closely similar to xanthate **1** but blue-shifted in comparison to **3**. The N^N complexes **4** and **5** show a charge transfer band with extinction coefficients in the range of 2,000–6,000 M^{-1} cm^{-1}, similar to other copper-based carbene metal amide complexes.[3,14,16] These are assigned to ligand-metal-ligand charge transfer (LMLCT) processes (Figure 4).

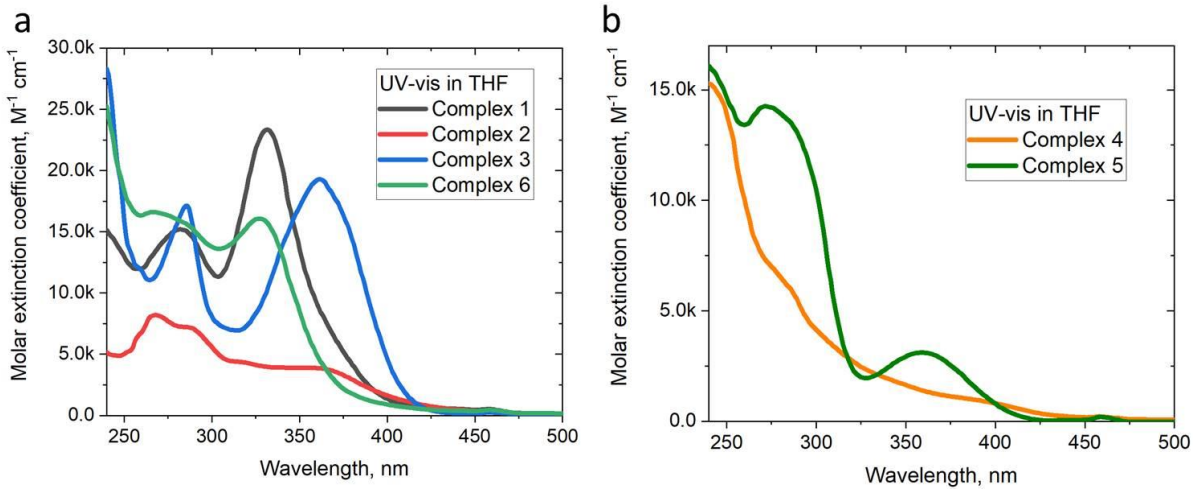

Figure 4. UV-Vis spectra for copper complexes with S^S and N^S ligands (a) and N^N ligands (b).

Neither the S^S nor the S^N complexes **1** – **3** show photoluminescence (PL) on excitation with various wavelength while complex **6** is very poorly emissive. This contrasts, for example, with the intense photoluminescence observed for three-coordinate P^P, S ligated copper thiolate complexes.[18] Excitation with wavelengths of 320–430 nm at 298 K compound **4**, with a distorted three-coordinate structure, gives bright yellow emission at 585 nm and photoluminescence quantum yield (PLQY) of 63.5%. The two-coordinate complex **5** shows a broad green-white emission with a solid state quantum yield of near-100% (Table 1 and Figure 5). Complex **4** with a hemilabile bidentate N-ligand complements therefore the numerous examples of photoemissive three-coordinate copper carbene complexes with chelating N-donor ligands.[19-23]

At 298 K crystalline powders of **4** and **5** show excited state lifetimes in the range of 14 – 24 µs. Upon cooling to 77 K, the lifetimes increase by a factor of 2 – 3 (Figure 6), while the emission profile red-shifts only slightly, with narrowing of its half bandwidth (Figure 5). There was no difference in the emission profiles of **4** and **5** measured early and after a delay of 80 µs (see ESI, Fig. S2 for time-resolved emission spectra). These facts indicate that the main emission pathway is phosphorescence in the solid state; the comparatively small increase in lifetimes at 77 K is likely associated with suppression of excited state relaxation modes.

Complexes **4** and **5** show significantly improved PLQY values while excited state lifetimes are much shorter compared with parent complexes (^{Me2}L)Cu(amide).[3,10] This is likely due to improved steric protection of the copper atom provided by the bulky guanidinate and formamidinate ligands with 2,6-diisopropylphenyl substituents.

Next we examined the PL behaviour in solution. In toluene complexes **4** and **5** are very weakly emissive at room temperature and produce orange and warm-white emissions, respectively. Complex **5** shows a shoulder around 600 nm which could be explained by the geometric flexibility of the formamidine ligand in solution enabling short contacts of N3 atom with copper. The triplet energy of the phosphorescent emitters was estimated by measuring the PL in frozen toluene. Complexes show high emission intensity leading to bright yellow **4** and white **5** luminescence with triplet energies of 2.27 and 2.55 eV, respectively.

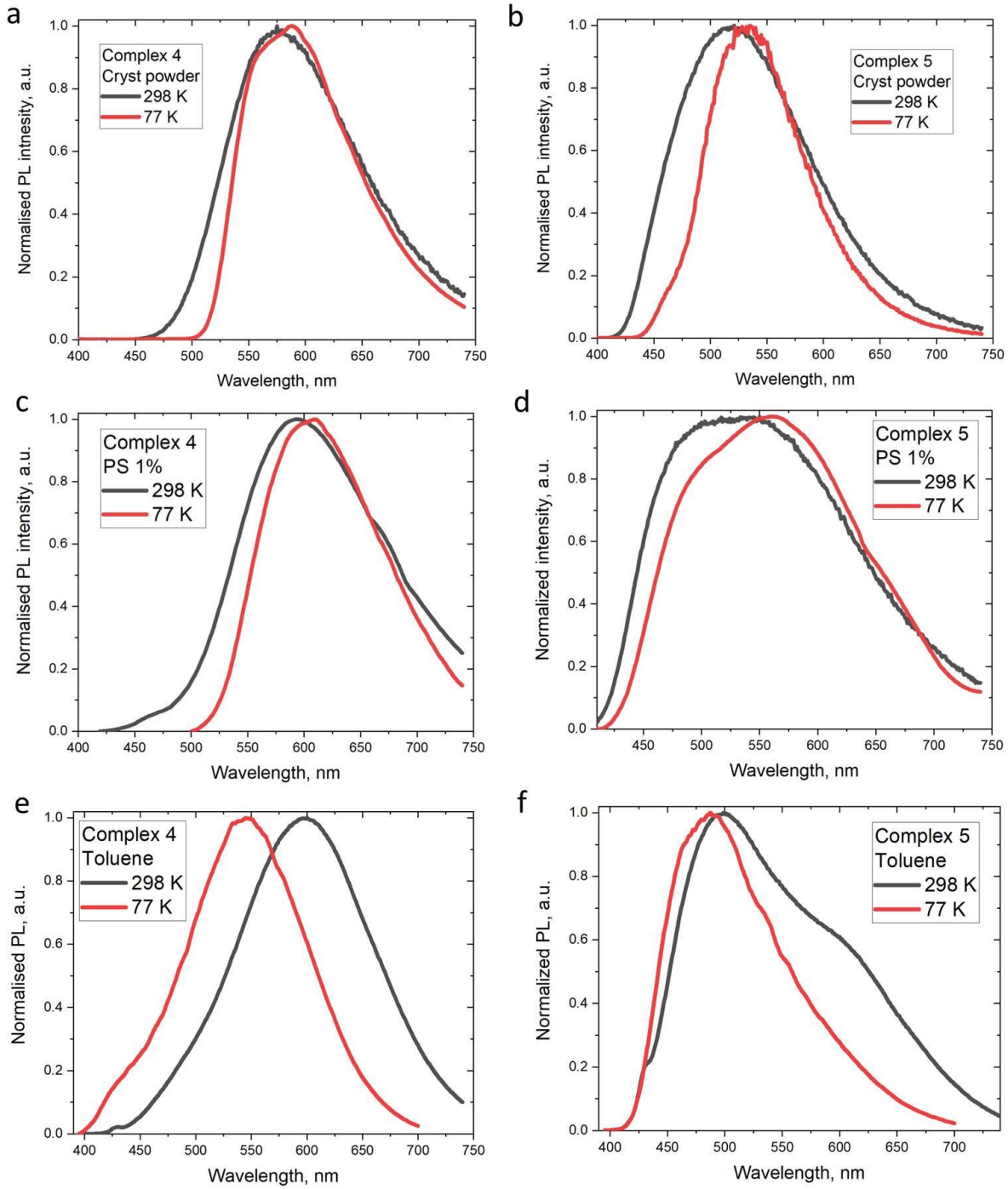

Figure 5. Photoluminescence spectra (298 and 77 K) excited at 380 nm under a nitrogen atmosphere: a) crystalline powder (**4**); b) crystalline powder (**5**); c) polystyrene film at a loading of 1 wt-% of **4**; d) polystyrene film at a loading of 1 wt-% of **5**; e) toluene solution at 298 K for **4** and **5**; f) toluene glass at 77 K for **4** and **5**.

Films of complexes embedded in a polystyrene (PS) matrix were prepared by drop-casting solutions onto a quartz substrate under nitrogen. To avoid concentration quenching processes, a low doping level of 1 weight-% was used to investigate the emissive properties

of **4** and **5**. When excited with 365 nm UV-light, complex **4** emits orange light at 570 nm, while a very broad warm-white emission is observed for complex **5** (Figure 5). This warm white emission of **5** is in line with the large values of full width at the half maximum (FWHM) of over 7000 cm^{-1}. The PS films show a behaviour similar to crystalline samples and on cooling to 77 K the excited state lifetimes increase up to three-fold. The PLQY values are reduced to 2 and 24% for **4** and **5**, respectively, compared to the PLQYs of the neat powders (Table 1). Unlike crystalline samples in which the molecules are held in a rigid matrix, amorphous polymer hosts likely permit some structural flexibility in the excited state, opening additional non-radiative pathways and resulting in lower PLQY values.

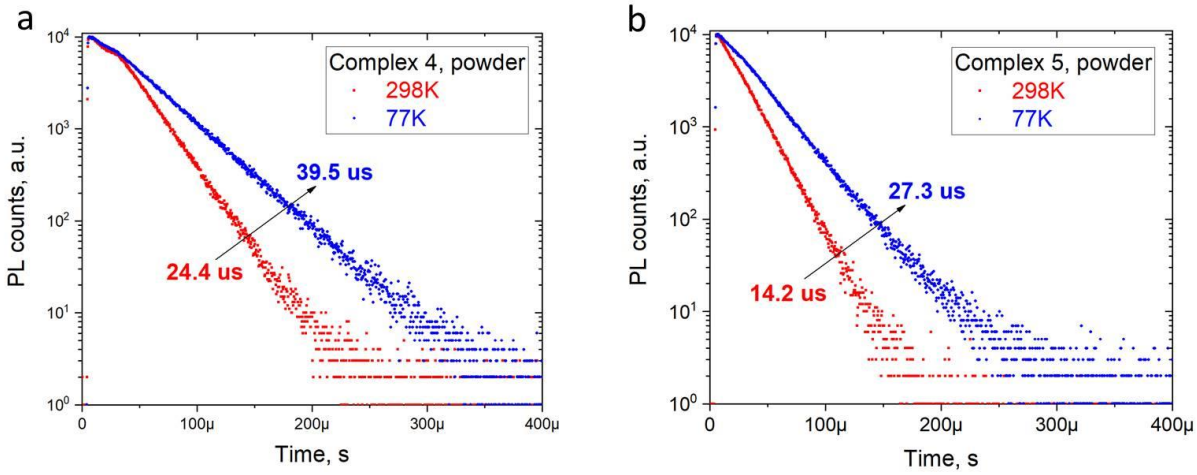

Figure 6. Photoluminescence decay profiles for complexes **4** and **5** at 298 and 77 K.

Table 1. PL data for **4** and **5** as crystalline powders, in toluene solution and as 1 wt-% dopants in PS films at 298 K and 77 K (values in parentheses).

	4			**5**		
	Powder	Toluene	PS[a] matrix	Powder	Toluene	PS[a] matrix
λ_{em} (nm)	577 (587)	598 (545)	592 (607)	518 (531)	500 (485)	520 (560)
τ (µs)	24.4[c] (39.5)	0.54[c]	11.1[c] (36.2)	14.2 (27.3)	1.9[c]	12.5[c] (30.3)
Φ(%, 300K; N_2)	63.5	–	2	96.6	–	24
k_r (10^4 s^{-1})	2.8	–	0.2	6.8	–	1.9
k_{nr} (10^4 s^{-1})	1.6	–	9.3	0.2	–	6.0
FWHM (cm^{-1}/ nm)	3959/ 136	4109/ 145	4227/ 155	5283/ 144	6198/ 175	7067/ 203

T_1 (eV) [b]	2.27	2.55

[a] Polystyrene films (1% by weight) were drop-cast from 10 mg/mL toluene solutions on a quartz substrate and evaporated under reduced pressure in a nitrogen-filled glove box chamber; [b] Triplet energy levels based on the emission max peak value in toluene glass at 77 K; [c] Two-component lifetime, τ average was used: $\tau_{av} = (B_1/(B_1 + B_2))\tau_1 + (B_2/(B_1 + B_2))\tau_2$, where B_1 and B_2 are relative amplitude for τ_1 and τ_2 , respectively.

Cyclic voltammetry has been used to estimate HOMO and LUMO energy levels for **4** and **5** (THF solution, $[^n Bu_4N]PF_6$ as supporting electrolyte; see Table 2 and ESI Figure S2). Both complexes show an irreversible reduction process with no back peak at all scan rates. The estimated LUMO energies for **4** (–2.43 eV) and **5** (–2.40 eV) are significantly destabilized due to the strong donor properties of the guanidinato and formamidinato ligands compared with chloride in the starting material (^{Me2}L)CuCl (–2.82 eV).[3] Both complexes show three irreversible oxidation waves with a substantial cathodic shift for complex **5** which correlates with lower donor properties of the formamidinate *vs* guanidinate. The HOMO levels based on the onset of the first oxidation potentials are -5.20 and -5.44 eV for **4** and **5**, respectively.

Table 2. Formal electrode potentials (peak position E_p for irreversible and $E_{1/2}$ for quasi-reversible processes (*), *V*, *vs*. $FeCp_2$), onset potentials (*E*, *V*, *vs*. $FeCp_2$), peak-to-peak separation in parentheses for quasi-reversible processes (ΔE_p in mV), E_{HOMO}/E_{LUMO} (eV) and band gap values (ΔE, eV) for the redox changes exhibited by **4** and **5**.[a]

Complex	Reduction		E_{LUMO}	Oxidation				E_{HOMO}	ΔE
	E_{1st}	$E_{onset\ red}$	eV	E_{1st}	$E_{onset\ ox}$	E_{2nd}	E_{3rd}	eV	eV
4	–3.21	–2.96	–2.43	–0.07	–0.19	+0.16	+0.44	–5.20	2.77
5	–3.24	–2.99	–2.40	+0.19	+0.05	+0.68	+0.92	–5.44	3.04

[a] In THF solution, recorded using a glassy carbon electrode, concentration 1.4 m*M*, supporting electrolyte $[^n Bu_4N][PF_6]$ (0.13 *M*), measured at 0.1 V s^{-1}.

Conclusion

In conclusion, ^{Me2}CAAC copper(I) complexes with *N*-, *S*,*S* and *S*,*N* donor ligands show coordination geometries that vary from strongly chelating to hemilabile and to linear-monodentate, with consequent changes in photophysical behaviour. The X-ray crystal structures show significant differences between guanidinato and formamidinato compounds, with the former displaying a long-range interaction to the second N-atom of the anion to give a distorted T-shaped three-coordinate geometry. The S^S chelate complexes **1**–**3** are air stable but thermally labile; on heating (^{Me2}L)Cu(S_2C-Cz) **3** eliminates CS_2 to form the carbazolato complex (^{Me2}L)Cu(Cz) quantitatively. The S-bound complexes **1**–**3** and **6** are non-emissive, whereas the N-bonded compounds are highly emissive in the crystalline state and show yellow (**4**) and green-white (**5**) phosphorescence with PLQYs of up to 96.6%. Polystyrene films show yellow (**4**) and warm-white emission (**5**) with PLQY up to 24% for **5**. The combination of the sterically less-hindered dimethyl-substituted CAAC-carbene ligand with bulky guanidinato and formamidinato ligands has enabled the synthesis of efficient photoemissive compounds with triplet energies in the range of 2.2–2.5 eV. The excited state lifetimes are of the order of 11–24 μs in the solid state and increase up to three-fold on cooling to 77K, thus indicating phosphorescence as a major emission pathway for complexes **4** and **5**. This contrasrt with the behaviour of previously reported CMA emitters which show delayed fluorescence with excited state lifetime which on cooling increase by more than one order of magnitude. The introduction of flexible electron-rich N-donors such as formamidinate extends the range of CMA molecular design towards efficient white light emitters.

Experimental

General Considerations. Unless stated otherwise all reactions were carried out in air. Solvents were distilled and dried as required. The carbene ligand ^{Me2}CAAC and the subsequent ^{Me2}CAACCuCl complex were obtained according to literature procedures.[24] ^{1}H and ^{13}C{^{1}H} NMR spectra were recorded using a Bruker Avance DPX-300 MHz NMR spectrometer and referenced to CD_2Cl_2 at δ 5.32 (^{13}C, δ 53.84), C_6D_6 at δ 7.16 (δ ^{13}C 128.06) and THF-d_8 at 3.58 (δ ^{13}C 67.21) ppm. Potassium *tert*-butoxide, N,N′-bis(2,6-di*iso*propylphenyl) formamidine**,** sodium 1,3-dithio-2-diethyl carbamate, sodium ethylxanthate and thioacetanilide were obtained from Sigma Aldrich. The compounds sodium 1,3-dithio-2-carbazolylcarbamate,[25] 1,3-bis(2,6-di*iso*propylphenyl)-2-dimethylguanidine[26] were prepared according to literature procedures. All electrochemical experiments were performed using an Autolab PGSTAT 302N computer-controlled potentiostat. Cyclic

voltammetry (CV) was performed using a three-electrode configuration consisting of either a glassy carbon macrodisk working electrode (GCE) (diameter of 3 mm; BASi, Indiana, USA) combined with a Pt wire counter electrode (99.99 %; GoodFellow, Cambridge, UK) and an Ag wire pseudoreference electrode (99.99 %; GoodFellow, Cambridge, UK). The GCE was polished between experiments using alumina slurry (0.3 μm), rinsed in distilled water and subjected to brief sonication to remove any adhering alumina microparticles. The metal electrodes were then dried in an oven at 100 °C to remove residual traces of water, the GCE was left to air dry and residual traces of water were removed under vacuum. The Ag wire pseudoreference electrodes were calibrated to the ferrocene/ferrocenium couple in MeCN at the end of each run to allow for any drift in potential, following IUPAC recommendations.[27] All electrochemical measurements were performed at ambient temperatures under an inert argon atmosphere in THF containing the complex under study (1.4 m*M*) and supporting electrolyte [n-Bu_4N][PF_6] (0.13 *M*). Data were recorded with Autolab NOVA software (v. 1.11). Elemental analyses were performed by London Metropolitan University. UV-visible absorption spectra were recorded using a Perkin-Elmer Lambda 35 UV/vis spectrometer. Photoluminescence measurements in toluene were recorded on a Fluorolog Horiba Jobin Yvon spectrofluorometer. Photoluminescence measurements of crystalline powders, PS films, time-resolved emission spectra, photoluminescence quantum yields were recorded using an integrating sphere on an Edinburgh Instruments FS5 spectrofluorometer under nitrogen atmosphere. The emission decays for powder samples and PS films were collected on an Edinburgh Instruments FS5 spectrofluorometer using the 5 W microsecond Xe flashlamp with a repetition rate of 100 Hz (excitation at 380 nm). Time resolved fluorescence data for toluene solutions were collected on a time-correlated single photon counting (TCSPC) Fluorolog Horiba Jobin Yvon spectrofluorimeter using Horiba Jobin Yvon DataStation v2.4 software. A NanoLED of 370 nm was used as excitation source, with an instrument response function width of 2 ns. The collected data were analysed using a Horiba Jobin Yvon DAS6 v6.3 software. TGA-DSC analysis was performed using a Mettler-Toledo TGA-DSC, using a small amount of sample (approx. 5 mg). A background measurement, using an empty 70 μL platinum pan, was taken initially, over a 50–600 °C temperature range.

Synthesis of (^{Me2}CAAC)Cu(ethylxanthate) (1)

An oven-dried round-bottomed flask was equipped with a stirring bar and charged with potassium ethylxanthate (65 mg, 0.40 mmol) and (^{Me2}CAAC)CuCl (155 mg, 0.40 mmol). Ethanol (20 mL) was added and the solution was stirred for 2 h at room temperature,

resulting in a yellow solution. Volatiles were evaporated under vacuum. The solid residue was extracted with dichloromethane and the supernatant filtered through a glass frit. Volatiles were evaporated using a rotary evaporator to give a brown solid. The product was crystallized from CH_2Cl_2/hexane. Yield: 140 mg (0.30 mmol, 74 %).

^{1}H NMR (300 MHz, CD_2Cl_2): δ 7.42 (t, *J* = 7.7 Hz, 1H, CAAC 4-C_6H_3 aromatic), 7.27 (d, *J* = 7.7 Hz, 2H, CAAC 3,5-C_6H_3 aromatic), 4.31 (q, *J* = 7.1 Hz, 2H, CH_2Me), 2.89 (sep, *J* = 6.7 Hz, 2H, CAAC $CHMe_2$), 2.04 (s, 2H, CAAC CH_2), 1.51 (s, 6H, CAAC CH_3), 1.34 (s, 6H, CAAC CH_3), 1.31 – 1.25 (m, *J* = 6.8 Hz, 15H, CH_3) ppm. ^{13}C NMR (75 MHz, CD_2Cl_2): δ 231.4 (C carbene), 145.8 (*o*-C), 135.4 (C_{ipso}), 129.4 (*p*-CH), 124.9 (*m*-CH), 81.1 (C_q), 70.9 (O<u>*C*</u>H_2), 55.0 (C_q), 50.0 (CH_2), 29.4 (CH_3), 29.3 (CH_3), 27.0 (CH), 22.9 (CH_3), 14.2 (OCH_2<u>*C*</u>H_3) ppm. Anal. Calcd. for $C_{23}H_{36}CuNOS_2$ (470.21): C, 58.75; H, 7.72; N, 2.98; S, 13.64. Found: C, 59.02; H, 7.97; N, 3.11; S, 13.34.

Synthesis of (^{Me2}CAAC)Cu(1,3-dithio-2-diethylcarbamate) (2)

An oven-dried round-bottomed flask was equipped with a stirring bar and charged with sodium 1,3-dithio-2-diethyl carbamate (102 mg, 0.45 mmol) and (^{Me2}CAAC)CuCl (153 mg, 0.40 mmol). Ethanol (30 mL) was added and the solution was stirred for 1 h at room temperature resulting in a green solution. Volatiles were evaporated using a rotary evaporator. The solid was taken with dichloromethane and filtered through a glass frit. The product was crystallized from CH_2Cl_2/hexane to give an orange solid. Yield: 182 mg (0.37 mmol, 91%).

^{1}H NMR (300.13 MHz, CD_2Cl_2) δ 7.41 (t, *J* = 9.3 Hz, 1H, CAAC 4-C_6H_3 aromatic), 7.26 (d, *J* = 7.7 Hz, 2H, CAAC 3,5-C_6H_3 aromatic), 3.76 (q, *J* = 7.1 Hz, 4H, CH_2Me), 2.89 (sep, *J* = 6.8 Hz, 2 H, CAAC $CHMe_2$), 2.00 (s, 2H, CAAC CH_2), 1.51 (s, 6H, CAAC CH_3), 1.31 (s, 6H, CAAC CH_3), 1.28 (d, *J* = 6.6 Hz, 12H, CAAC CH_3), 1.16 (t, *J* = 7.1 Hz, 6H, CH_3) ppm. ^{13}C NMR (75 MHz, CD_2Cl_2): δ 208.5 (C carbene), 145.8 (*o*-C), 135.5 (C_{ipso}), 128.7 (*p*-CH), 124.5 (*m*-CH), 80.0 (C_q), 54.6 (N<u>*C*</u>H_2), 50.0 (C_q), 47.0 (CH_2), 29.5 (CH_3), 29.1 (CH_3), 26.7 (CH), 22.8 (CH_3), 12.9 (NCH_2<u>*C*</u>H_3) ppm. Anal. Calcd. for $C_{25}H_{41}CuN_2S_2$ (497.28): C, 60.38; H, 8.31; N, 5.63; S, 12.89. Found: C, 60.44; H, 8.22; N, 5.72; S, 13.00.

Synthesis of (^{Me2}CAAC)Cu(1,3-dithio-2-carbazolyl carbamate) (3)

An oven-dried Schlenk flask was equipped with a stirring bar and charged with sodium 1,3-dithio-2-carbazolate carbamate (196 mg, 0.46 mmol) and (^{Me2}CAAC)CuCl (178 mg, 0.46 mmol) under an argon atmosphere. Anhydrous dichloromethane (10 mL) was added and the

mixture was stirred for 1 h at room temperature resulting in a deep red solution. The mixture was filtered through a glass frit with a plug of Celite. All volatiles were evaporated to give the product as a red solid. Yield: 200 mg (0.34 mmol, 73 %).

^{1}H NMR (300 MHz, CD_2Cl_2) δ 9.02 (d, *J* = 8.4 Hz, 2H, Carbazole 1-C_6H_4), 7.94 (d, *J* = 7.4 Hz, 2H, Carbazole 4-C_6H_4), 7.43 (d, *J* = 3.4 Hz, 1H, CAAC 3,5-C_6H_3), 7.40 (t, *J* = 7.2 Hz, 2H, CAAC 4-C_6H_3), 7.32 (t, *J* = 7.5 Hz, 4 H, Carbazole 2,3-C_6H_4), 2.98 (sept, *J* = 6.8 Hz, 2H, CAAC $CHMe_2$), 2.08 (s, 2H, CAAC CH_2), 1.59 (s, 6H, CAAC CH_3), 1.38 – 1.32 (m, *J* = 6.8 Hz, 18H, CAAC CH_3) ppm. ^{13}C NMR (75 MHz, CD_2Cl_2): δ 221.5 (C carbene), 145.7 (*o*-C), 140.5 ($S_2\underline{C}N$), 135.2 (C_{ipso}), 129.1 (*p*-CH), 126.3 (*m*-CH), 126.1 (*m*-CH), 124.6 (*2*-CH), 123.3 (*3*-CH), 119.1 (*1*-CH), 118.2 (*4*-CH), 80.7 (C_q), 54.6 (C_q), 49.8 (CH_2), 29.2 (CH_3), 29.1 (CH_3), 26.9 (CH), 22.7 (CH_3) ppm. Anal. Calcd. for $C_{33}H_{39}CuN_2S_2$ (591.36): C, 67.03; H, 6.65; N, 4.74; S, 10.84. Found: C, 66.88; H, 6.90; N, 4.71; S, 10.53.

CS_2 elimination reaction to give (^{Me2}CAAC)Cu(carbazolate). Complex **3** (200 mg, 0.34 mmol) was heated under vacuum at 180 °C for 10 min. The initial deep-red melt converted to dark-brown after 5 min, with evaporation of CS_2. After cooling, ^{1}H and ^{13}C{^{1}H} NMR experiments confirmed the clean formation of (^{Me2}CAAC)Cu(carbazolate) which was recrystallized by layering a toluene solution with hexane. Yield: 154 mg (0.30 mmol, 88 %). The ^{1}H NMR spectrum of this product proved to be identical to that previously reported.[10]

Synthesis of (^{Me2}CAAC)Cu(1,3-bis(2,6-di*iso*propylphenyl)-2-dimethylguanidinate) (4)

An oven-dried Schlenk flask was equipped with a stirring bar and charged with 1,3-bis(2,6-di*iso*propylphenyl)-2-dimethyl guanidine (251 mg, 0.62 mmol), (^{Me2}CAAC)CuCl (266 mg, 0.69 mmol) and potassium *tert*-butoxide (85 mg, 0.76 mmol) under an argon atmosphere. Anhydrous diethyl ether (25 mL) was added and the mixture was stirred for 4 h at room temperature. The resulting yellow solution was filtered through a cannula under an argon atmosphere. Volatiles were evaporated under vacuum, affording a bright yellow solid. Yield: 420 mg (0.56 mmol, 89 %).

^{1}H NMR (300 MHz, C_6D_6): δ 7.26 (d, *J* = 7.4 Hz, 4H, dipp), 7.14 (m, *J* = 7.2 Hz, 3H, CAAC aromatic), 6.98 (d, *J* = 7.7 Hz, 2H, dipp aromatic), 4.02 (sep, *J* = 6.8 Hz, 4H, dipp $CHMe_2$), 2.73 (sep, *J* = 6.7 Hz, 2 H, CAAC $CHMe_2$), 2.34 (s, 6H, NCH_3), 1.52 (s, 6H, CAAC CH_3), 1.47 (d, *J* = 6.9 Hz, 12H, CAAC CH_3), 1.41 (s, 2H, CAAC CH_2), 1.30 (d, *J* = 6.7 Hz, 12H, dipp CH_3), 1.13 (d, *J* = 6.8 Hz, 12H, dipp CH_3), 0.81 (s, 6H, CAAC CH_3) ppm. ^{13}C NMR (75 MHz, C_6D_6): δ 252.1 (C carbene), 164.4 (DippN–$\underline{C}NMe_2$=NDipp), 147.5 (N-C_{ipso},

guanidine), 145.2 (*o*-C), 141.7 (*o*-C, guanidine), 135.0 (C_{ipso}), 129.3 (*p*-CH), 124.7 (*m*-CH), 123.0 (*m*-CH, guanidine), 121.1 (*p*-CH, guanidine), 80.4 (C_q), 55.4 (C_q), 49.8 (CH_2), 39.8 ($N\underline{Me}_2$), 29.1 (CH_3), 28.8 (CH_3), 27.4 (CH_3), 27.0 (CH), 25.5 (CH), 23.4 (CH_3), 22.4 (CH_3) ppm. Anal. Calcd. for $C_{47}H_{71}CuN_4$ (755.66): C, 74.71; H, 9.47; N, 7.41. Found: C, 74.95; H, 9.62; N, 7.39.

Synthesis of (^{Me2}CAAC)Cu(N,N′-bis(2,6-di-isopropylphenyl)formamidinate) (5)

An oven-dried Schlenk flask was equipped with a stirring bar and charged with N,N′-bis(2,6-di-isopropylphenyl) formamidine (153 mg, 0.42 mmol), (^{Me2}CAAC)CuCl (161 mg, 0.42 mmol) and potassium *tert*-butoxide (60 mg, 0.54 mmol) under an argon atmosphere. Dry diethyl ether (20 mL) was added and the solution was stirred for 4 h at room temperature resulting in a colourless solution. The solution was filtered through a cannula under an argon atmosphere. Volatiles were removed under vacuum, affording an off-white solid. Yield: 260 mg (0.36 mmol, 87 %).

^{1}H NMR (300.13 MHz, THF-d_8) δ 7.33 (t, *J* = 6.6 Hz, 1H, CAAC 4-C_6H_3 aromatic), 7.23 (d, *J* = 7.1 Hz, 2H, CAAC 3,5-C_6H_3 aromatic), 6.99 (s, 1H, CH), 6.84 (d, *J* = 7.1 Hz, 4H, dipp 3,5-C_6H_3 aromatic), 6.75 (t, *J* = 7.1 Hz, 2H, dipp 4-C_6H_3 aromatic), 3.51 (sep, *J* = 6.9 Hz, 4H, dipp $CHMe_2$), 2.88 (sep, *J* = 6.8 Hz, 2 H, CAAC $CHMe_2$), 2.06 (s, 2H, CAAC CH_2), 1.57 (s, 6H, CAAC CH_3), 1.32 (s, 6H, CAAC CH_3), 1.26 (d, *J* = 6.7 Hz, 6H, CAAC CH_3), 1.06 (d, *J* = 6.8 Hz, 6H, CAAC CH_3), 1.02 (d, *J* = 6.9 Hz, 24H, dipp CH_3) ppm. ^{13}C NMR (75 MHz, THF-d_8): δ 251.6 (C carbene), 161.9 (DippN–$\underline{C}$H=NDipp), 148.9 (N-C_{ipso}, formamidine), 145.8 (*o*-C), 143.1 (*o*-C, formamidine), 135.3 (C_{ipso}), 130.1 (*p*-CH), 125.1 (*m*-CH), 122.4 (*m*-CH, formamidine), 122.2 (*p*-CH, formamidine), 81.8 (C_q), 55.3 (C_q), 49.9 (CH_2), 29.7 (CH_3), 29.0 (CH_3), 28.7 (CH_3), 27.9 (CH), 27.0 (CH), 24.0 (CH_3), 22.3 (CH_3) ppm. Anal. Calcd. for $C_{45}H_{66}CuN_3$ (712.59): C, 75.85; H, 9.34; N, 5.90. Found: C, 75.47; H, 9.22; N, 6.08.

Synthesis of (^{Me2}CAAC)Cu(thioacetanilide) (6)

An oven-dried Schlenk flask was equipped with a stirring bar and charged with thioacet-anilide (57 mg, 0.37 mmol, 1 eq.), (^{Me2}CAAC)CuCl (144 mg, 0.37 mmol, 1 eq.) and potassium *tert*-butoxide (55 mg, 0.49 mmol, slight excess) under an argon atmosphere. Anhydrous diethyl ether (35 mL) was added and the mixture was stirred for 4 h at room temperature. The resulting yellow solution was filtered through a cannula under an argon atmosphere. Volatiles were removed under vacuum, affording a yellow solid. Yield: 131 mg (0.26 mmol, 64 %).

^{1}H NMR (300.13 MHz, CD_2Cl_2) δ 7.42 (t, *J* = 8.0 Hz, 1H, CAAC 4-C_6H_3 aromatic), 7.28 (d, *J* = 7.7 Hz, 2H, CAAC 3,5-C_6H_3 aromatic), 7.19 (t, *J* = 8.0 Hz, 2H, 3,5-C_6H_3 aromatic), 6.91 (t, *J* = 7.4 Hz, 1H, 4-C_6H_3 aromatic), 6.62 (d, *J* = 7.3 Hz, 2H, 2,6-C_6H_3 aromatic), 2.85 (sep, *J* = 7.3 Hz, 2 H, CAAC $CHMe_2$), 2.04 (s, 2H, CAAC CH_2), 1.45 (s, 6H, CAAC CH_3), 1.36 (s, 6H, CAAC CH_3), 1.31 (d, *J* = 6.7 Hz, 12H, CAAC CH_3) 1.23 (s, 3H, CH_3) ppm. ^{13}C NMR (75 MHz, CD_2Cl_2): δ 249.6 (C carbene), 172.4 (C=S), 154.5 (C_{ipso}, thioacetanilide), 145.5 (*o*-C), 135.0 (C_{ipso}), 129.9 (*p*-CH), 128.6 (*m*-CH, thioacetnilide), 125.1 (*m*-CH), 122.2 (*p*-CH, acetanilide), 120.9 (*o*-CH, thioacetanilide), 81.1 (C_q), 54.6 (C_q, overlapping with residual solvent signal), 49.8 (CH_2), 38.0 (CH_3, thioacetanilide), 29.4 (CH_3), 29.3 (CH_3), 28.6 (CH_3), 27.1 (CH), 22.6 (CH_3) ppm. Anal. Calcd. for $C_{28}H_{39}CuN_2S$ (499.24): C, 67.36; H, 7.87; N, 5.61; S, 6.42. Found: C, 67.46; H, 7.94; N, 5.37; S, 6.66.

Conflicts of interest

There are no conflicts to declare.

Acknowledgement.

This work was supported by the European Research Council and the Royal Society. M. B. is an ERC Advanced Investigator Award holder (grant no. 338944-GOCAT). A. S. R. acknowledges support from the Royal Society (grant nos. URF\R1\180288 and RGF\EA\181008).

† Electronic supplementary information (ESI) contains UV , PL and electrochemical and X-ray crystallographic data. CCDC 1915487 for **3**, 1915489 for **4**, and 1915488 for **5**. For ESI and crystallographic data in CIF or other electronic format see DOI: XXXXX

§ Dedicated to Professor Annie Powell on the occasion of her 60th birthday.

References

1 A. S. Romanov, D. Di, Le Yang, J. Fernandez-Cestau, C. R. Becker, C. E. James, B. Zhu, M. Linnolahti, D. Credgington, and M. Bochmann, *Chem. Commun*. 2016, **52**, 6379 – 6382 and *Chem. Commun*., 2018, **54**, 3672.

2 D. Di, A. S. Romanov, L. Yang, J. M. Richter, J. P. H. Rivett, S. Jones, T. H. Thomas, M. Abdi Jalebi, R. H. Friend, M. Linnolahti, M. Bochmann, and D. Credgington, *Science* 2017, **356**, 159–163.

3 A. S. Romanov, C. R. Becker, C. E. James, D. Di, D. Credgington, M. Linnolahti, and M. Bochmann, *Chem. Eur. J.* 2017, **23**, 4625–4637.

4 A. S. Romanov and M. Bochmann, *J. Organomet. Chem*. 2017, **847**, 114-120.

5 P. J. Conaghan, S. M. Menke, A. S. Romanov, A. J. Pearson, E. W. Evans, M. Bochmann, N. C. Greenham, and D. Credgington, *Adv. Mater*. 2018, **30**, 1802285.

6 C. R. Hall, A. S. Romanov, M. Bochmann and S. R. Meech, *J. Phys. Chem. Lett*. 2018, **9**, 5873–5876.

7 A. S. Romanov, S. T. E. Jones, L. Yang, P. J. Conaghan, D. Di, M. Linnolahti, D. Credgington and M. Bochmann, *Adv. Optical Mater*. 2018, **6**, 1801347.

8 M. Gernert, U. Meller, M. Haehnel, J. Pflaum and A. Steffen, *Chem. Eur. J*. 2017, **23**, 2206-2216.

9 R. Hamze, R. Jazzar, M. Soleilhavoup, P. I. Djurovich, G. Bertrand and M. E. Thompson, *Chem. Commun.* 2017, **53**, 9008-9011.

10 R. Hamze, J. L. Peltier, D. Sylvinson, M. C. Jung, J. Cardenas, R. Haiges, M. Soleilhavoup, R. Jazzar, P. I. Djurovich, G. Bertrand, and M. E. Thompson, *Science* 2019, **363**, 601-606.

11 S. Shi, M. C. Jung, C. Coburn, A. Tadle, D. Sylvinson M. R., P. I. Djurovich, S. R. Forrest, and M. E. Thompson, *J. Am. Chem. Soc*. 2019, **141**, 3576−3588.

12 J. Föller and C. M. Marian, *J. Phys. Chem. Lett*. 2017, **8**, 5643-5647.

13 E. J. Taffet, Y. Olivier, F. Lam, D. Beljonne, and G. D. Scholes, *J. Phys. Chem. Lett.* 2018, **9**, 1620−1626.

14 S. Thompson, J. Eng and T. J. Penfold, *J. Chem. Phys*. 2018, **149**, 014304.

15 (a) H. Yersin, (ed).. Wiley-VCH, Weinheim, 2019. **ISBN:** 978-3-527-33900-6; (b) H. Yersin, R. Czerwieniec, M. Z. Shafikov, and A. F. Suleymanova, *ChemPhysChem* 2017, **18**, 3508-3535. (c) M. J. Leitl, D. M. Zink, A. Schinabeck, T. Baumann, D. Volz, and H. Yersin, *Top. Curr. Chem.* **2016,** *374*, 25.

16 (a) A. Kurek, P.G. Gordon, S. Karle, A. Devi, B. S.T. Barry, *Aust. J. Chem*., 2014, **67**, 989–996; (b) O. Seitz, M. Dai, F.S. Aguirre-Tostado, R.M. Wallace, Y.J. Chabal, *J. Am. Chem. Soc.*, 2009, **131**, 18159–18167.

17 J. Casanova, G. Alzuet, J. Borras, O. Carugo, *J. Chem. Soc. Dalton Trans*. 1996, 2239; CCDC1549332 and CCDC1549334.

18 M. Osawa, *Chem. Commun*. 2014, **50**, 1801-1803.

19 M. Osawa, M. Hoshino, M. Hashimoto, I. Kawata, S. Igawa and M. Yashima, *Dalton Trans.* 2015, **44**, 8369-8378.

20 M. Hashimoto, S. Igawa, M. Yashima, I. Kawata, M. Hoshino, and M. Osawa, *J. Am. Chem. Soc.* 2011, **133**, 10348-10351.

21 V. A. Krylova, P. I. Djurovich, M. T. Whited and M. E. Thompson, *Chem. Commun*. 2010, **46**, 6696–6698.

22 M. J. Leitl, V. A. Krylova, P. I. Djurovich, M. E. Thompson and H. Yersin, *J. Am. Chem. Soc*. **2014**, *136*, 16032−16038.

23 R. Marion, F. Sguerra, F. DiMeo, E. Sauvageot, J. F. Lohier, R. Daniellou, J. L. Renaud, M. Linares, M. Hamel and S. Gaillard, *Inorg. Chem*. **2014**, *53*, 9181-9191.

24 H. Braunschweig, W. C. Ewing, T. Kramer, J. D. Mattock, A. Vargas, and C. Werner, *Chem. Eur.J.*2015, **21**,12347 –12356.

25 N. Azizi, F. Aryanasab, and M. R. Saidi, *Org. Lett.* 2006, **8**, 5275-5277.

26 R. Green, A. C. Walker, M. P. Blake, P. Mountford, *Polyhedron* 2016, **116**, 64-75.

27 G. Gritzner, J. Kůta, *Electrochim. Acta* 1984, **29**, 869-873.